Supporting Information

Deciphering alcohol dehydrogenase catalysis in glycerol-based deep eutectic solvents through experimental and computational insights

Ningning Zhang,[†a] Jan Philipp Bittner,[†b] Aaron Pfleger,[b] Pablo Domínguez de María,[c] Sven Jakobtorweihen,[b,d] Irina Smirnova,[*b] Selin Kara[*a,e]

[a] Institute of Technical Chemistry
Leibniz University Hannover
Callinstraße 5, 30167 Hannover, Germany
E-mail: selin.kara@iftc.uni-hannover.de

[b] Institute of Thermal Separation Processes
Hamburg University of Technology
Eißendorfer Straße 38, 21073 Hamburg, Germany

[c] Sustainable Momentum, SL.
Av. Ansite 3, 4-6, 35011, Las Palmas de Gran Canaria, Canary Islands, Spain

[d] Department for Chemical Reaction Engineering
Hamburg University of Technology
Eißendorfer Straße 38, 21073 Hamburg, Germany
E-mail: irina.smirnova@tuhh.de

[e] Biocatalysis and Bioprocessing Group, Department of Biological and Chemical Engineering
Aarhus University
Gustav Wieds Vej 10, 8000 Aarhus, Denmark
E-mail: selin.kara@bce.au.dk

[†] Both authors contributed equally to this work.

TABLE OF CONTENTS

1. Conversion of volume fraction and mole fraction for DES-water mixtures

For molecular dynamics (MD) simulations, the experimentally used volume fractions (vol.%) need to be transferred to ion-based mole fractions (x_i, mol.%). The conversion was conducted with

$$x_i = \frac{n_i}{n_{\text{cation}^+} + n_{\text{Cl}^-} + n_{\text{HBD}} + n_{\text{W}}} \qquad \textbf{(Eqn. 1)}^1$$

and the result is shown in **Table S1**.

Table S1. Conversion between volume fractions (vol.%) and mole fractions of water (mol.%, Xw)

Volume fraction [vol.% H_2O]	ChAc-Gly (1:2) Mole fraction [x_W (mol%)]	Bet-Gly (1:2) Mole fraction [x_W (mol%)]
0	0	0
5	17.8	20.4
10	31.5	35.1
20	50.8	54.9
30	63.9	67.6
40	73.4	76.5
50	80.5	83.0
60	86.1	87.9
70	90.6	91.9
80	94.3	95.1
90	97.4	97.8
95	98.7	98.9
100	100	100

2. Preparation and characterization of DESs

2.1 Preparation of DES and DES-buffer mixture

For Bet-Gly (1:2), betaine (0.2 mol, 24.43 g) and glycerol (0.4 mol, 36.84 g) were weighted in a sealed round flask and mixed at 80°C, 300 rpm for 2 h to obtain a clear liquid which was sealed and stored at room temperature for one week before further use.

For ChAc-Gly (1:2), choline acetate (0.2 mol, 32.64 g) and glycerol (0.4 mol, 36.84 g) were weighted in a sealed round flask and mixed at 80°C, 300 rpm for 2 h to obtain a clear slight yellowish liquid which was sealed and stored at room temperature for one week before further use.

To prepare DES-water and DES-buffer mixtures, ddH_2O or Tris-HCl (50 mM, pH 7.5) was added into the obtained DESs in the defined amount. After adding the buffer, the DES-buffer mixture was thoroughly mixed and stored overnight at room temperature for equilibration before use.

2.2 Water content

Water content (wt.%) of pure DES was determined by Karl Fischer Titration with TitroLine® 7750 (SI Analytics, Germany) based on the consumption of the HYDRANAL™ Composite 2 during a colorimetric titration.

2.3 Water activity

The 5 mL of freshly prepared DESs and DES-water mixtures were incubated in 30 mL sealed glass bottles at 25°C for 3 days. Afterwards, water activity (a_W), defined as on the ratio of the water vapor pressure (p) in the DES-water mixtures to the vapor pressure of pure water (p_0), was determined at room temperature using an HMT337 Humidity Sensor (Vaisala, Finland).

2.4 Dynamic viscosity

The determination of dynamic viscosity (η) of DESs and DES-water mixtures was performed by applying 750 µL samples to the Modular Compact Rheometer MCR302 by Anton Paar with a PP40 plate. The measurements were taken across shear rates of 1–60 s^{-1} at temperatures between 25°C and 45°C for the pure DESs. The shear rates for the 80 vol.% DES-water mixtures were adjusted to be 1–300 s^{-1}. All the measurements were conducted in duplicates.

3. Production and characterization of enzymes

3.1 Enzyme production

Horse liver alcohol dehydrogenase (HLADH) was produced by heterologous expression in *E. coli* BL21(DE3) carrying the plasmid pET28b(+)-HLADH-His with an N-terminal His-tag and kanamycin resistance according to the reported protocol.[1] *E. coli* cells from a glycerol stock was used to inoculate 30 mL LB medium with kanamycin (50 µg/mL) as preculture, which was incubated at 150 rpm and 37°C overnight. The main culture was inoculated in a 1:40 ratio by adding 25 mL preculture to 1 L LB medium with kanamycin (50 µg/mL) in a 5 L Erlenmeyer flask. The main culture was incubated at 37°C and 100 rpm for 2–3 h until OD_{600} reached 0.6−0.8. For induction, IPTG was added to reach a final concentration of 0.5 mM, and the incubation was continued at 100 rpm and 24°C for ~24 h. The cells were harvested by centrifugation at 8000 rpm and 4°C for 10 min. The obtained cell pellets were re-suspended in Tris-HCl buffer (20 mM, pH 7.5) at a ratio of 5 mL buffer per gram wet cells. The re-suspended cells were disrupted by ultrasonication (Sartorius Labsonic M with MS73 probe) on ice at 60% amplitude (4 sec. on, 6 sec. off, 2 min × 5 cycles with 2 min resting

on ice between each cycle). The water-soluble protein was separated from the cell debris by centrifugation at 13,000 rpm and 4°C for 45 min. The obtained clear cell-free extract (CFE) was filtrated through a 0.2 µm sterile filter and stored at 4°C for further purification.

Enzyme purification was conducted by utilizing the His-tag for immobilized metal ion affinity chromatography (IMAC) via nitrilotriacetate nickel (Ni-NTA) columns. The ÄKTA® Start system (Cytiva, the US) equipped with HisTrap™ HP column of 5 mL (column volume, CV) was used to load, wash, and elute samples with wash buffer (50 mM NaH_2PO_4, 300 mM NaCl, 20 mM imidazole, pH 8.0) and elution buffer (50 mM NaH_2PO_4, 300 mM NaCl, 250 mM imidazole, pH 8.0), respectively. All fractions from the purification step were kept at 4°C for further SDS-PAGE analysis. The desirable fractions were combined for further desalting followed by lyophilization.

3.2 Enzyme characterization

Bradford assay was performed by incubating 20 µL sample and 200 µL Bradford reagent in a 96-microwell plate at 25°C for 5 min. The absorption at 595 nm was measured at 25°C by Multiskan SkyHigh plate reader and applied to the calibration curve of BSA in a linear range up to 500 µg/mL.

SDS-PAGE was performed by using 12 vol.% gel and running at 180 V for 1 h. All protein samples were diluted to desired concentrations, mixed with 4x Laemmli buffer, and heated at 95°C for 10 min before being loaded to the gel (**Figure S1**).

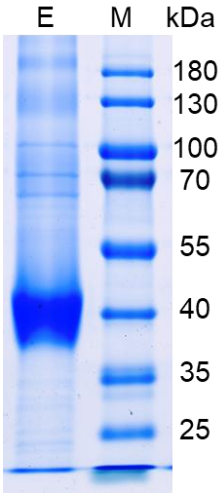

Figure S1. SDS-PAGE analysis of purified HLADH. E: purified enzyme solution. M: Marker.

4. Melting temperature of enzyme in DES-buffer systems

The melting temperature of enzymes was determined with Nano Differential Scanning Fluorimetry (NanoDSF, NanoTemper). The measurement was conducted with 1 mg/mL protein in 100 µL DES-buffer mixtures containing varying buffer contents (5–90 vol.%, Tris-HCl, 50 mM, pH 7.5) (**Tables S2**) across a temperature range of 20−95°C at a ramp of 1°C/min. The fluorescence ratio at 350/330 nm was recorded upon protein unfolding (**Figure S2**), the first derivative of which can be obtained as the melting temperature under the specific conditions (**Figures 2a**).

Table S2. Components in the DES-buffer systems containing varying buffer contents (5–90 vol.%, Tris-HCl, 50 mM, pH 7.5) for melting temperature analysis.

Buffer content [vol.%]	DES [µL]	Tris-HCl buffer [µL]	Enzyme stock in buffer [µL]
5	95	0	5
10	90	5	5
20	400	15	5
30	350	25	5
40	300	35	5
50	250	45	5
60	200	55	5
70	150	65	5
80	100	75	5
90	50	85	5
100	0	95	5

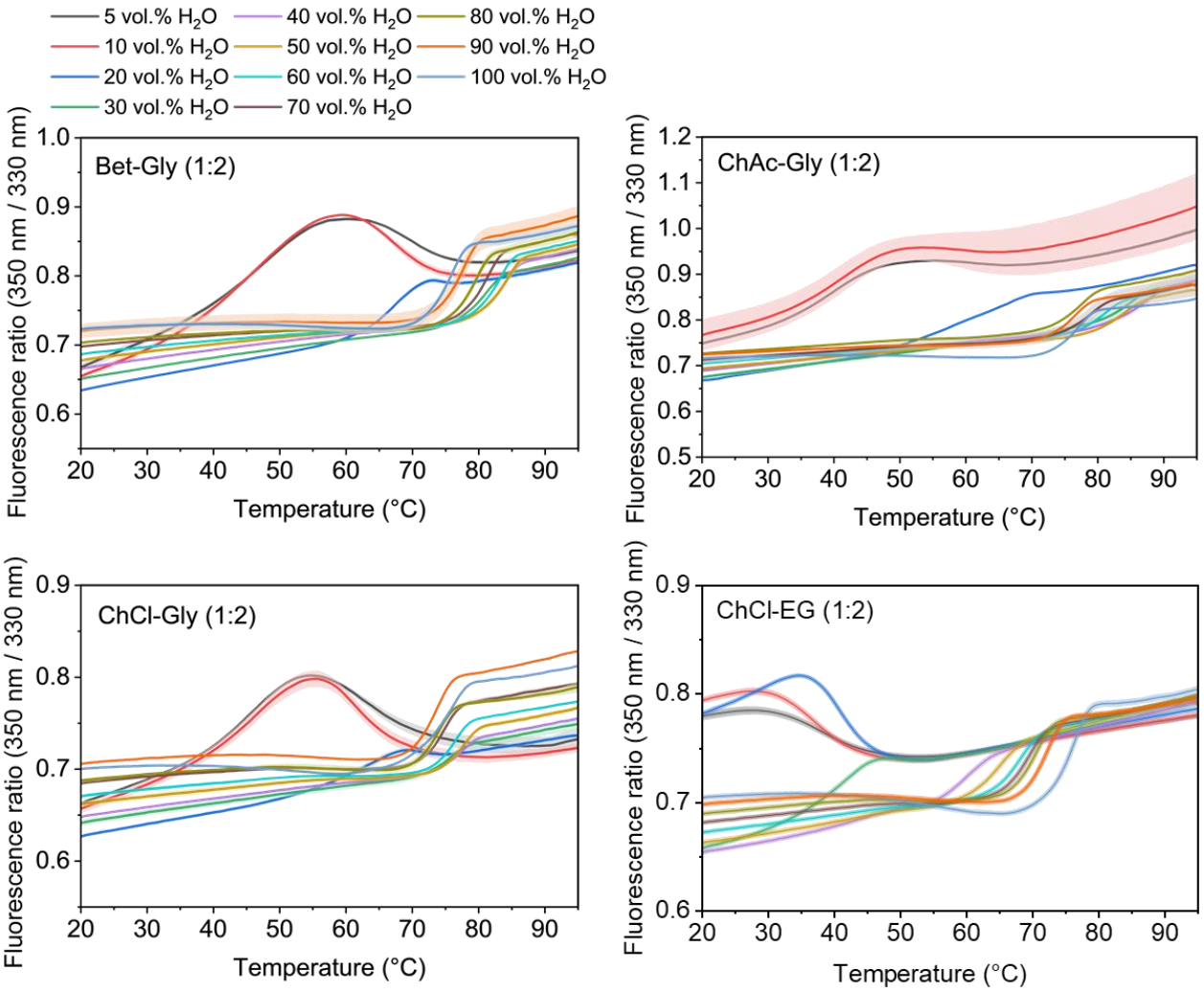

Figure S2. Thermal unfolding profiles of purified HLADH in DES-buffer systems containing varying water contents (5–90 vol.%, Tris-HCl, 50 mM, pH 7.5) with the pure buffer system (100 vol.%) as reference, across a temperature range of 20−95°C at a ramp of 1°C/min. All results are based on triplicate experiments with shaded error bars.

5. Half-life time of enzyme in DES-buffer systems

The half-life times of enzymes were determined by incubating 500 µL of 1.0 mg/mL purified HLADH at 60°C in DES-buffer mixtures containing varying buffer contents (5–90 vol.%), referring to the pure buffer system. The corresponding incubation media were put in 1.5-mL plastic tubes and kept at room temperature overnight for equilibration (**Table S3**). Then, 25 µL enzyme solution (20 mg/mL) was mixed with the above-equilibrated solution and incubated at 60°C. Aliquot samples were taken at defined time intervals, and the residual activities were measured at 25°C with the standard photometric assay. The half-life time was determined from the plots of the natural logs of residual activities versus the incubation time, and calculated based on

$$t_{1/2} = \frac{\ln 2}{k_d} \quad \text{(Eqn. 2)}$$

where $t_{1/2}$ represents the half-life time [min]

and k_d the deactivation constant [min^{-1}]. Each reaction was performed in duplicates.

Table S3. Components in the DES-buffer systems containing varying buffer contents (5–90 vol.%, Tris-HCl, 50 mM, pH 7.5) for half-life time analysis.

Buffer content [vol.%]	DES [µL]	Tris-HCl buffer [µL]	Enzyme stock in buffer [µL]
5	475	0	25
10	450	25	25
20	400	75	25
30	350	125	25
40	300	175	25
50	250	225	25
60	200	275	25
70	150	325	25
80	100	375	25
90	50	425	25
100	0	475	25

6. Specific activity of enzyme with photometric assay

6.1 Spectroscopic analysis

UV–Visible spectroscopy was performed with a 1 mL system in a Quartz cuvette at 25°C using a Cary 60 spectrophotometer (Agilent Technologies, the US). The spectral scanning was performed in the wavelength range of 200–800 nm for Tris-HCl buffer (50 mM, pH 7.5), DESs, DES-buffer mixtures, and DES-buffer mixtures with reaction (see **Figure S3**).

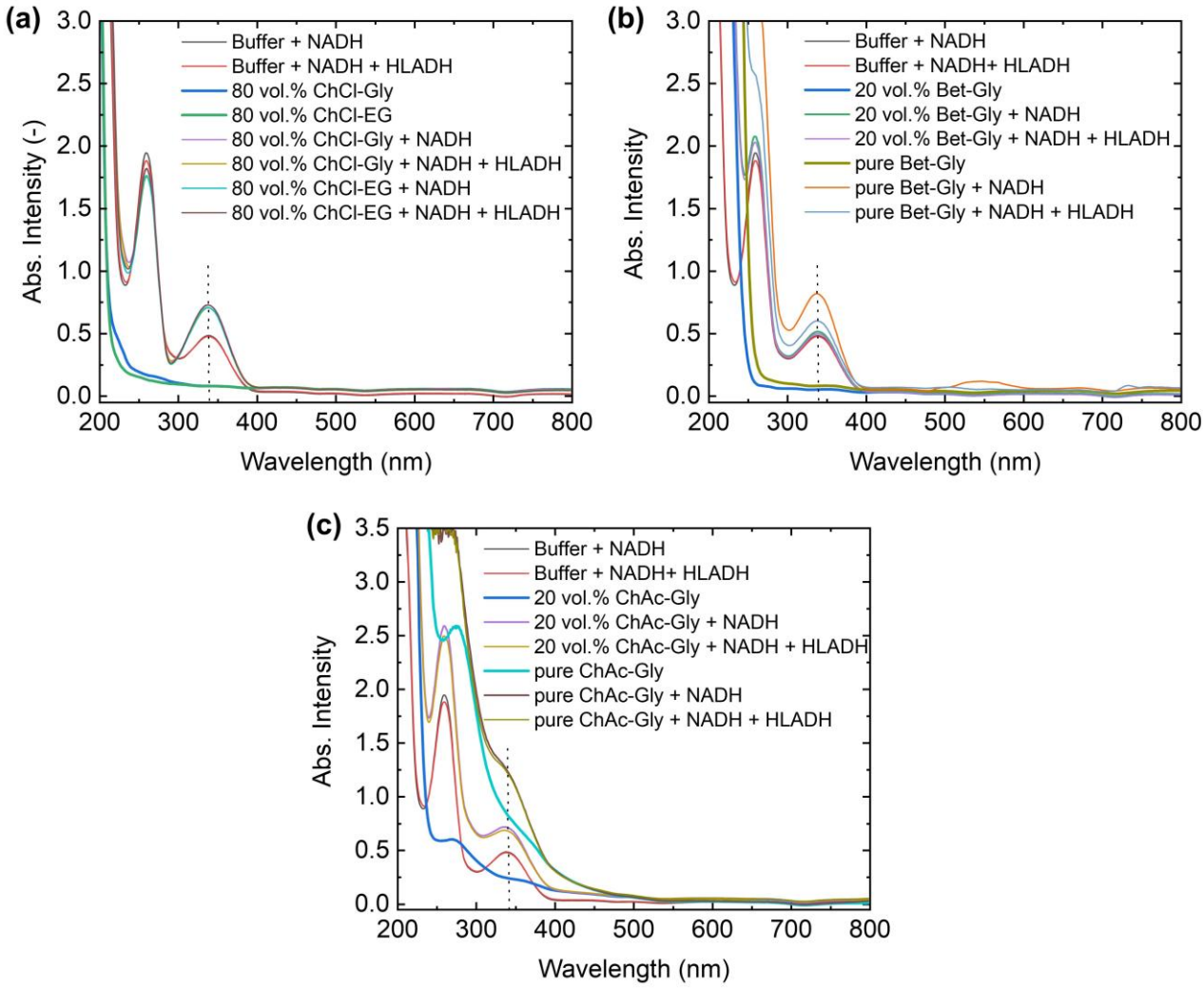

Figure S3. Spectral analysis of DES-buffer mixtures containing NADH or/and HLADH: (a) ChCl-Gly (1:2) and ChCl-EG (1:2), (b) Bet-Gly (1:2), and (c) ChAc-Gly (1:2).

6.2 Photometric assay

The specific activity of HLADH was determined by monitoring the depletion of NADH at 340 nm using Cary 60 Spectrophotometer (Agilent Technologies, the US). The reaction was monitored at 25°C for 1 min, and the slope of the linear trend was taken to calculate the specific activity. The standard photometric reaction was carried out in a 1 mL Tris-HCl buffer system (50 mM, pH 7.5) containing cyclohexanone (CHO, 50 mM), NADH (0.1 mM), and a defined amount of HLADH.

7. Catalytic performance of enzyme in cascade reaction with GC analysis

The reactions were performed in 1 mL pure buffer and DES-buffer systems containing varying buffer contents (0–90 vol.%) at 1000 rpm and 25°C. The DES-buffer reaction systems (**Table S4**) were

prepared by mixing DES, buffer, substrate, and cosubstrate, in 1.5 mL GC vials, and incubated at 25°C overnight for equilibration. The lyophilized enzymes were dissolved in buffer (Tris-HCl, 50 mM, pH 7.5), and NADH was added to obtain enzyme/NADH stock solutions to start the reaction. The reaction system contains CHO (50 mM), 1,4-BD (25 mM), NADH (0.1 mM), and HLADH (1 mg/mL).

Table S4. Components in the DES-buffer systems containing varying buffer contents (5–90 vol.%, Tris-HCl, 50 mM, pH 7.5) for enzyme activity analysis.

Buffer content [vol.%]	DES [µL]	Tris-HCl buffer [µL]	Enzyme and NADH stock in buffer [µL]
0%	1000	0	0
5%	950	0	50
10%	900	50	50
20%	800	150	50
30%	700	250	50
40%	600	350	50
50%	500	450	50
60%	400	550	50
70%	300	650	50
80%	200	750	50
90%	100	850	50
100%	0	950	50

GC sample preparation and analysis

Samples were taken at the defined times and prepared for GC analysis. For this, 50 µL reaction mixture was taken to 250 µL ethyl acetate (EtOAc) containing 2 mM methyl benzoate (MB) in a 1.5 mL tube. The mixture was vortexed for 30 sec and centrifuged at 13,400 rpm for 2 min to obtain a phase separation. The organic phase was taken and dried with anhydrous $MgSO_4$ followed by a 2 min of centrifuging at 13,400 rpm before transferring to GC vials. The GC analysis was performed using Nexis GC-2030 with AOC-20i Plus auto injector (SHIMADZU). The details of the GC method are shown in **Table S5** and **Figure S4.** The reaction was analyzed and quantified based on the respective calibration curves regarding mass balance, yield, and specific activity.

Table S5. The parameters of GC analytic methodology for HLADH-catalyzed CHO cascade.

Heating program			Column	Analysis result	
Rate [°C/min]	T [°C]	Hold [min]		Component	t_R [min]
-	80	0	CP-ChiraSil -DEX CB 25 m x 0.25 mm x 0.25 µm	CHO	5.98
10	160	0		GBL	6.14
30	190	3		CHL	7.02
				MB	7.82
				1,4-BD	9.02

T (Injector): 250°C; Detector: FID; *T* (Detector): 275°C; Carrier gas: H_2;
Column flow: 0.65 mL min^{-1}; Total flow: 24 mL min^{-1}; Split ratio: 30.
EtOAc: ethyl acetate, 1,4-BD: 1,4-butanediol, GBL: γ-butyrolactone, CHO: cyclohexanone, CHL: cyclohexanol, MB: methyl benzoate

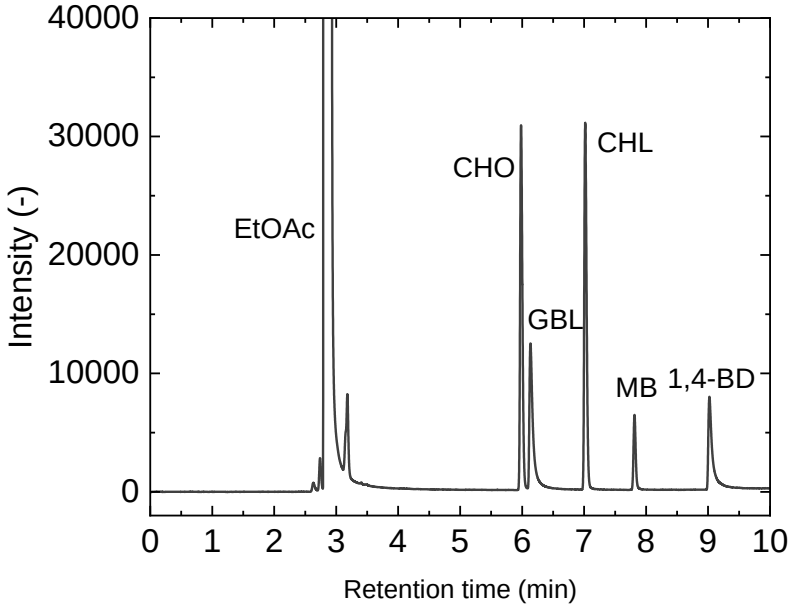

Figure S4. Gas chromatogram of all the reaction components of HLADH-catalyzed cyclohexanone reduction.

8. Performance of enzyme in individual DES-buffer systems

8.1 Melting temperature

The same procedure described in **Section 4** was used for the melting temperature analysis. The measurement was conducted with 1 mg/mL protein in 100 µL DES-buffer mixtures containing 40 vol.% or 60 vol.% buffer contents (Tris-HCl, 50 mM, pH 7.5) (**Tables S6**).

Table S6. Components in the systems containing DES individual components and different buffer contents (Tris-HCl, 50 mM, pH 7.5) for melting temperature analysis. The conversion of vol.% to mol% in ChAc-Gly (1:2) and Bet-Gly (1:2) is found in **Table S1**.

System	Buffer content [vol.%]	Tris-HCl buffer [µL]	DES or individual DES component [mg or µL]	Enzyme stock in buffer [µL]
ChAc	40	30	52 mg	10
Gly	40	30	60 µL	10
ChAc-Gly (1:2)	40	30	60 µL	10
Bet	60	50	40 mg	10
Gly	60	50	40 µL	10
Bet-Gly (1:2)	60	50	40 µL	10
Pure buffer	100	90	/	10

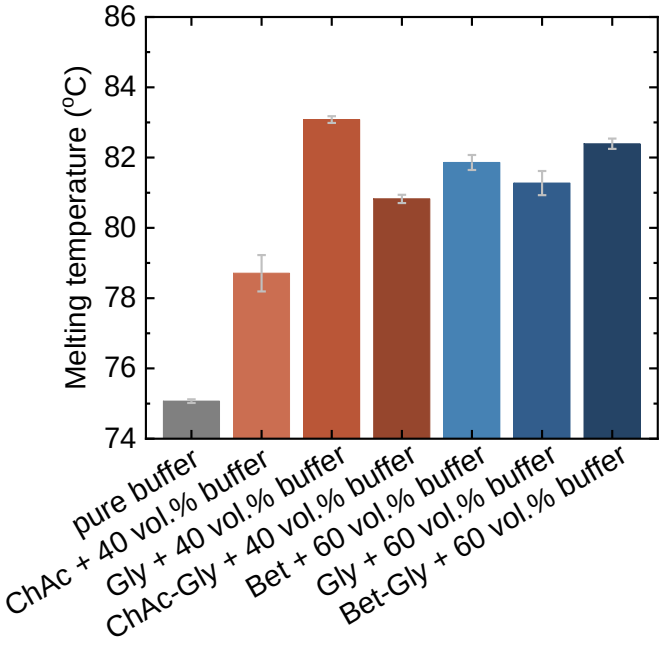

Figure S5. Melting temperature of purified HLADH in the systems of ChAc-Gly (1:2), Bet-Gly (1:2), and DES individual components with different buffer contents. All results are based on triplicate experiments.

8.2 Specific activity

The same procedure described in **Section 7** was used for specific activity analysis. The 0.5 mL individual DES-buffer reaction systems (**Table S7**) were prepared by mixing DES or DES individual components, buffer, substrate, and cosubstrate in 1.5 mL Eppendorf tubes.

Table S7. Components in the systems containing DES, individual components, and different buffer contents (Tris-HCl, 50 mM, pH 7.5) for enzyme activity analysis. The conversion of vol.% to mol.% in ChAc-Gly (1:2) and Bet-Gly (1:2) is found in **Table S1**.

System	Buffer content [vol.%]	Tris-HCl buffer [μL]	DES or DES individual component [mg or μL]	Enzyme and NADH stock in buffer [μL]
ChAc	40	150	257 mg	50
Gly	40	150	300 μL	50
ChAc-Gly (1:2)	40	150	300 μL	50
Bet	60	250	200 mg	50
Gly	60	250	200 μL	50
Bet-Gly (1:2)	60	250	200 μL	50
Pure buffer	100	450	/	50

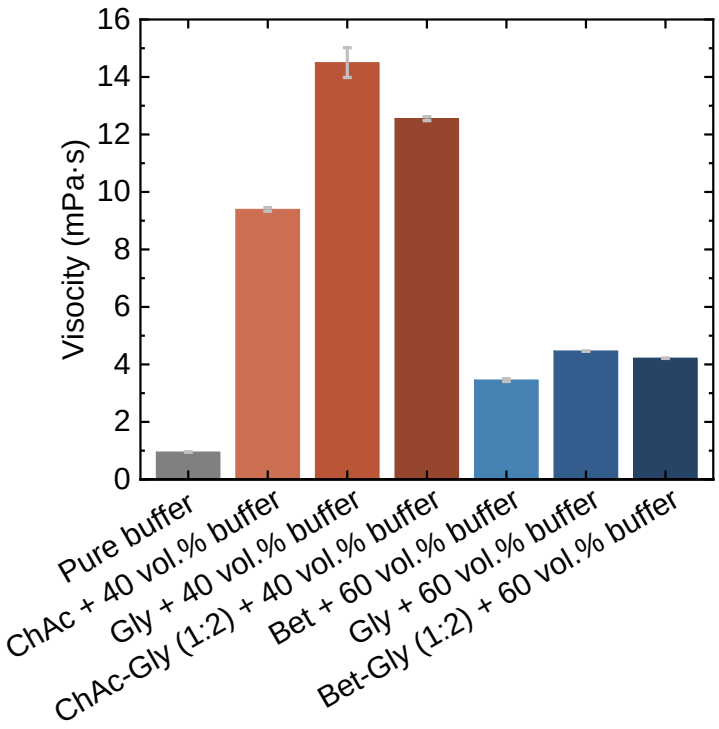

Figure S6. Dynamic viscosity of the reaction systems containing ChAc-Gly (1:2), Bet-Gly (1:2), DES individual components with different buffer contents (Tris-HCl, 50 mM, pH 7.5) at 25°C.

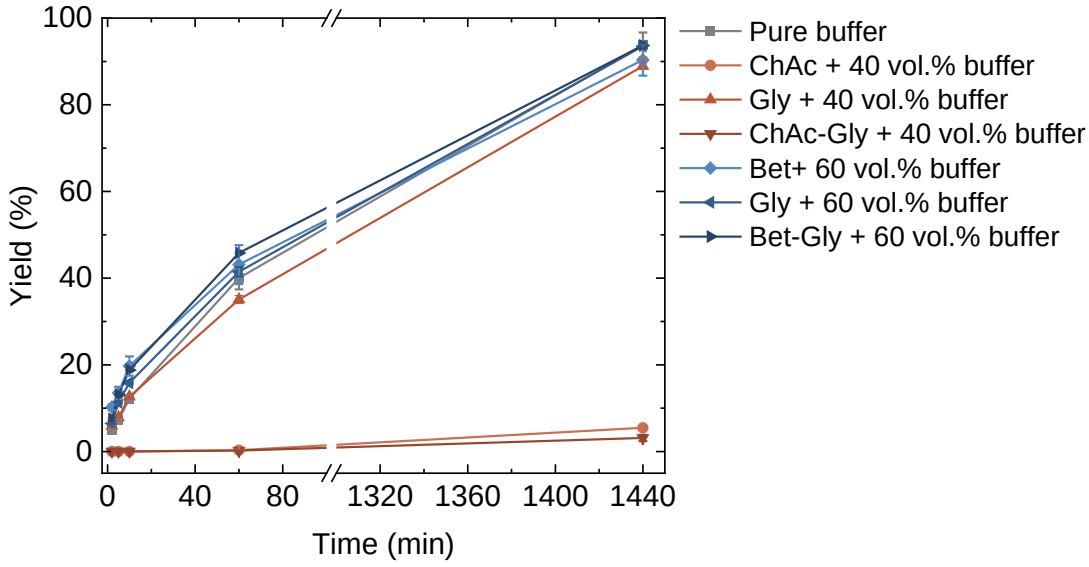

Figure S7. Reaction progress of HLADH-catalyzed reduction of cyclohexanone (CHO) to cyclohexanol (CHL) coupled with 1,4-butanediol (1,4-BD) for cofactor regeneration in the systems of ChAc-Gly (1:2), Bet-Gly (1:2), and DES individual components with different buffer contents (Tris-HCl, 50 mM, pH 7.5).

Table S8. pH values of mixtures of DESs and Tris–HCl buffer (50 mM, pH 7.5).

Mixtures of buffer and DESs or DES components	pH values
ChAc-Gly (1:2) + 20 vol.% buffer	7.47 ± 0.01
ChAc-Gly (1:2) + 40 vol.% buffer	6.78 ± 0.01
ChAc-Gly (1:2) + 60 vol.% buffer	6.33 ± 0.03
Bet-Gly (1:2) + 20 vol.% buffer	8.16 ± 0.01
Bet-Gly (1:2) + 40 vol.% buffer	7.87 ± 0.01
Bet-Gly (1:2) + 60 vol.% buffer	7.74 ± 0.01

9. Computational analyses

The MD simulations of this work were conducted using the GROMACS software package[2-4] versions 2019.6 and 2022.5. GROMACS is a simulation package that has been optimized for biomolecules.

9.1 Force fields

The HLADH structure was modeled in this work using the CHARMM36m force field[5] as of March 2019. The force field models, topologies, and parameters for all DES molecules were obtained from the CHARMMGUI[6-9] using CHARMM general force field (CGenFF) version 4.1.[10, 11] The water molecules are modeled using the TIP3P-CHARMM variant.[12] In a previous publication,[13] the combination of CGenFF for polar and charged DES molecules in combination with the CHARMM protein force field and CHARMM variant for water was already tested. Despite its inability to accurately reflect the dynamic properties of the DES/water mixtures at low water contents, which can be mitigated by increasing the water content, this combination can adequately represent the structural and energetic properties of DES/water mixtures.

9.2 MD simulations

In this study, we conducted three distinct types of MD simulations. To validate the force field set-up for the DESs of this work, a set of solvent-only MD simulations was constructed. The density, thermodynamic water activity, and dynamic viscosity were subsequently determined. The equilibration scheme for the solvent-only simulations is based on previous publications.[13, 14] Initially, cubic boxes containing the pure DESs or 50 mol.% mixtures with water are packed using packmol.[15] Subsequently, an energy minimization is conducted via the steepest descent algorithm. A 1 ns NVT simulation is performed using the velocity rescale thermostat ($\tau_T = 1\ \mathrm{ps}$)[16] to equilibrate the temperature to 298.15 K. The leap-frog algorithm[17] with a time step of 1 fs is used to integrate Newton's equations of motion. To surmount energy barriers during the equilibration process for the highly viscous DES systems, a temperature annealing scheme from Huang & Bittner et al.[14] is employed, followed by a 10 ns NPT equilibration using a time step of 2 fs. During this the pressure is adjusted to 1 bar using the Berendsen barostat ($\tau_P = 5\ \mathrm{ps},\ \kappa_T = 5 \times 10^{-5}\ \mathrm{bar}^{-1}$).[18] Subsequently, an NPT sampling is performed for 50 ns by switching the pressure control to Parinello-Rahman.[19] A more detailed description of the equilibration can be found in Bittner et al.[13] Based on the NPT sampling, two special simulation set-ups for determining the thermodynamic activity of water via free energy perturbation and the dynamic viscosity using the periodic perturbation method are performed. For a more comprehensive overview of these special MD simulations, please refer to the work of Bittner et al.[13]

Furthermore, MD simulations with a single HLADH molecule are performed to assess its structural and solvation properties in different DES/water mixtures. Starting from the horse-liver alcohol

dehydrogenase structure (HLADH, PDB entry 1HET[20]), periodic cubic boxes (~14 nm) with the respective solvent compositions were assembled using PACKMOL,[15] preserving 46 internal water molecules to aid protein equilibration[21]. The equilibration protocol, adapted from previous studies,[13, 14] began with energy minimization via the steepest descent algorithm, followed by velocity assignment from a Maxwell-Boltzmann distribution. A 2 ns NVT equilibration used the velocity rescale thermostat[16] ($\tau_T = 1\ \mathrm{ps}$) to set the temperature to 298.15 K, with numerical integration of Newton's equations of motion by the leap-frog algorithm[22] (1 fs time step). Hydrogen atoms of water were constrained using SETTLE,[23] and all other bonds were constrained with LINCS.[24] Non-hydrogen atoms of HLADH were position-restrained to avoid structural distortion during the equilibration. To enhance the solvent equilibration around HLADH for the highly viscous DESs, temperature annealing raised the temperature to 500 K over 1 ns, maintained it for 20 ns, and cooled it back to 298.15 K within 1 ns. HLADH restraints were then gradually released over two 500 ps NVT simulations; first only the backbone and then only the C_α-atoms were restrained. A 2 ns NPT equilibration using the Berendsen barostat[18] ($\tau_P = 5\ \mathrm{ps},\ \kappa_T = 5 \times 10^{-5}\ \mathrm{bar}^{-1}$) adjusted the system pressure to 1 bar. The time step is from this point forward set to 2 fs. Finally, production simulations ran for 100 ns switching the pressure coupling to Parrinello-Rahman.[19] Thereby, the last 40 ns have been used to analyze enzyme/solvent properties using different GROMACS tools and snapshots of the MD simulations have been visualized using VMD.[25, 26]

Based on these simulations of a single and freely moving enzyme structure, umbrella sampling (US) simulations are performed to probe a substrate molecule along the binding tunnel of HLADH. Hereby, the exact set-up of Bittner et al.[27] is employed by creating 30 individual windows of a substrate molecule along the substrate binding tunnel with an umbrella distance of 0.1 nm. The substrate molecule is restrained along the reaction coordinate ζ with a harmonic potential ($\kappa_\zeta = 500\ \mathrm{kJ\ mol^{-1}nm^{-2}}$) and the lateral movement with the flat bottom potential with the same parameters as Bittner et al.[27] [27] In these simulations, the translational and rotational movement of the enzyme has been restrained while simultaneously retaining the internal degrees of freedom of the protein. The corresponding parameters and reasoning for the restraints can be found in Bittner et al.[27] In order to ensure a proper sampling of the entire tunnel replica exchange umbrella sampling (REUS)[28] is used with replica exchange attempts between neighboring umbrella windows every 1000 steps. To analyze the REUS simulations and construct free energy profiles along the binding tunnel, the Umbrella Integration (UI) method of Kästner and Thiel[29, 30] is used, which allows the determination of error bars by setting the error to zero in the bulk phase. For detailed information about the REUS set-up, please refer to Bittner et al.[27]

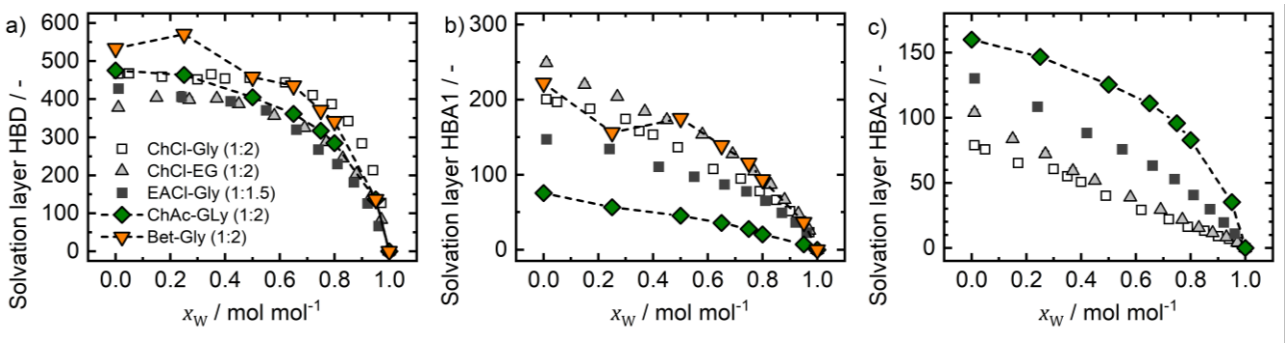

Figure S8. Solvation layer of DES and water molecules in direct contact with HLADH in the MD simulations for Bet-Gly (1:2) and ChAc-Gly (1:2) compared to ChCl-Gly (1:2), ChCl-EG (1:2) and EACl-Gly (1:1.5) from our previous study.[1] HBA1 represents a cation, while HBA2 represents an anion.

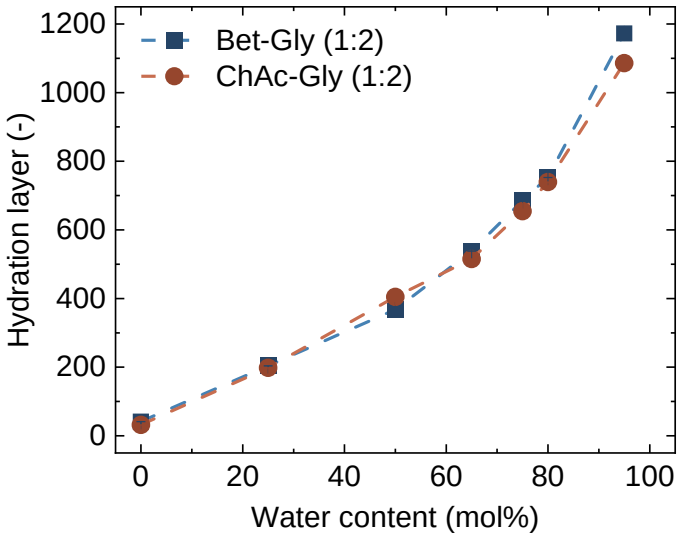

Figure S9. Hydration layers for Bet-Gly (1:2) and ChAc-Gly(1:2) from MD simulations. The conversion of mol% to vol.% in ChAc-Gly (1:2) and Bet-Gly (1:2) is found in **Table S1**.

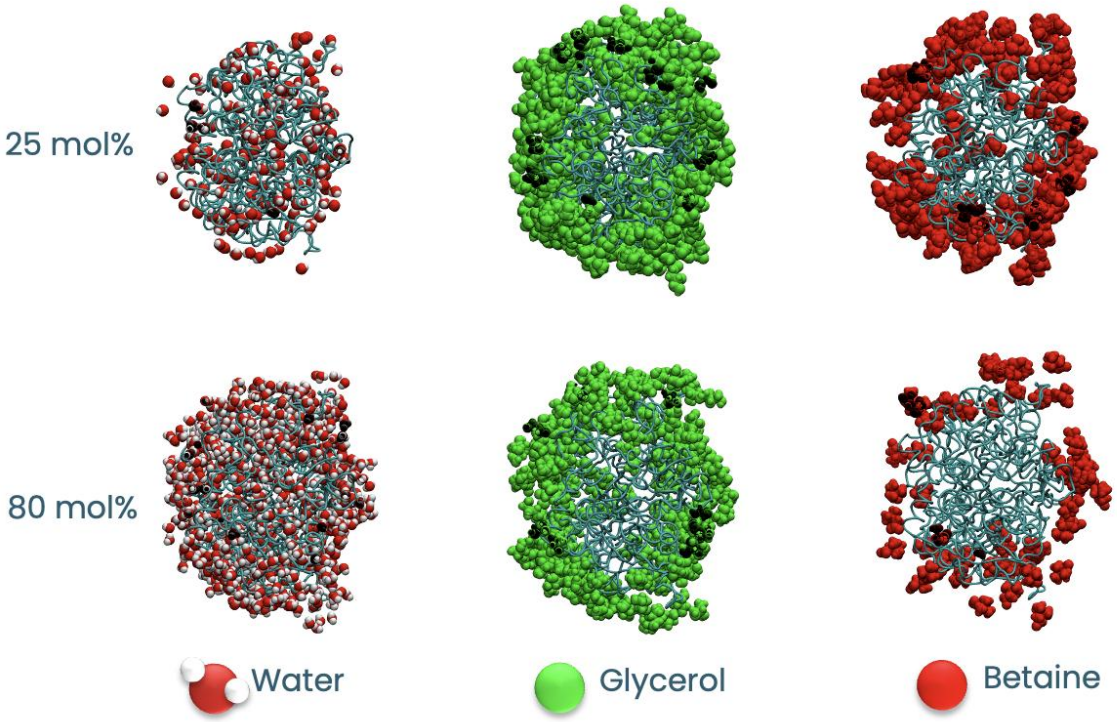

Figure S10. Solvation layers for the Bet-Gly (1:2) system at 25 mol% and 80 mol% water content.

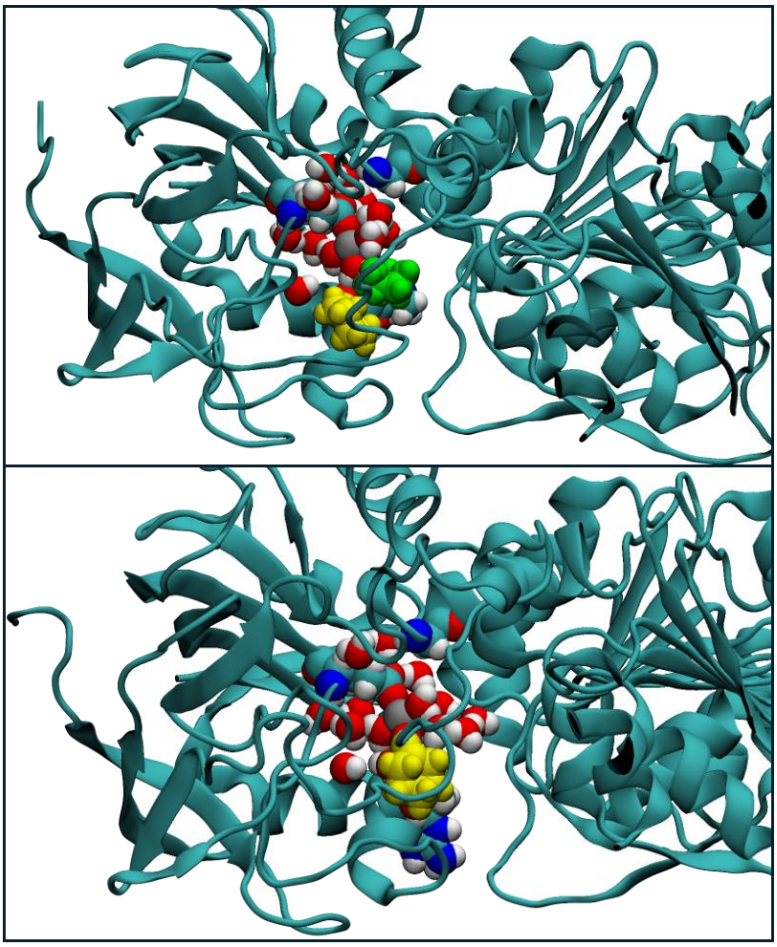

Figure S11. Snapshot of active center of replica 1 (bottom) and replica 2 (top) of Bet-Gly at 80 mol% water concentration at 50 ns of a 200 ns simulation. Cyclohexanone (yellow), glycerol (green), catalytic zinc-atom (grey), residues 46, 67, and 174, and water are represented as van der Waals spheres in VMD. Other residues and NADH are not shown for better visibility.

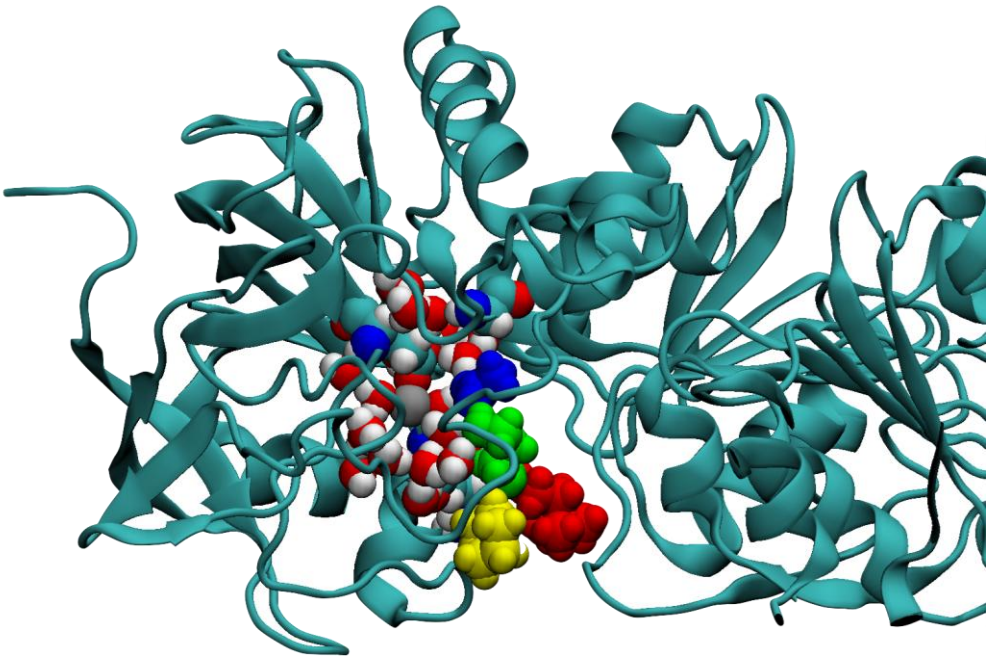

Figure S12. Snapshot of active center and substrate channel of replica 1 of ChAc-Gly at 75 mol% water concentration at 30 ns of a 100 ns simulation of umbrella window where the equilibrium position of cyclohexanone was fixed at 1.7 nm away from the active center. Cyclohexanone (yellow), glycerol (green), choline (red), acetate (blue), catalytic zinc atom (grey), residues 46, 67, and 174, and water are represented as van der Waals spheres in VMD. Other residues and NADH are not shown for better visibility.

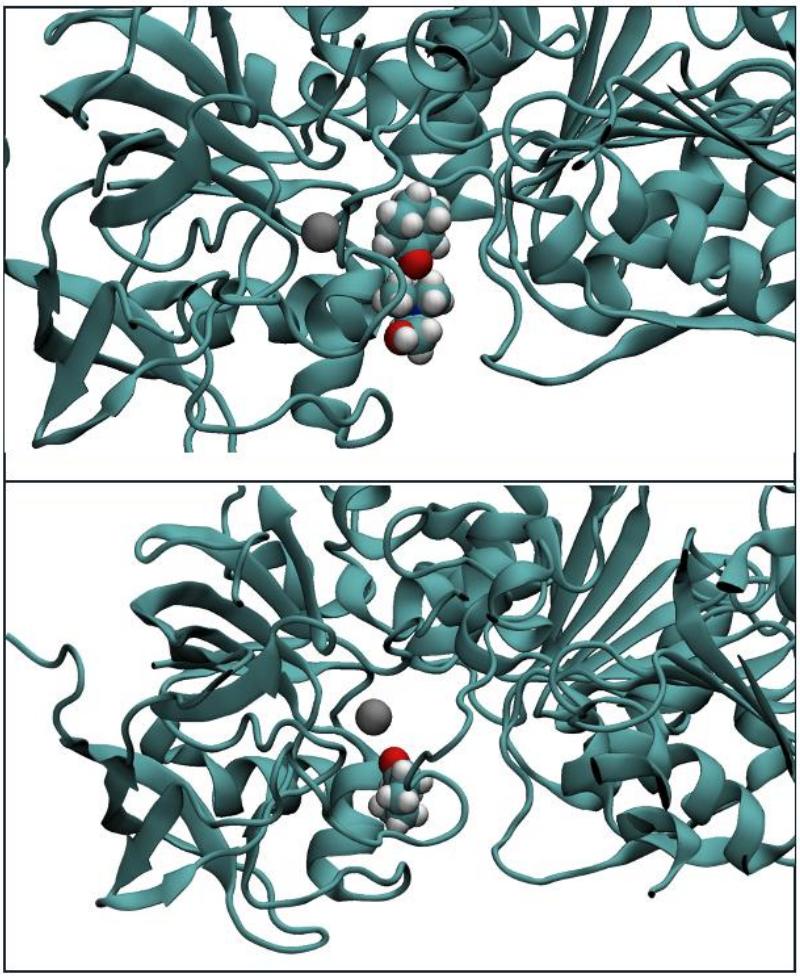

Figure S13. Snapshot of active center and substrate channel of replica 1 of ChAc-Gly at 75 mol% water concentration at 60 ns of a 100 ns simulation of umbrella window 10. Top figure shows cyclohexanone (top molecule) interacting with choline (bottom molecule) oriented away from zinc (grey). Bottom figure shows replica 2 with cyclohexanone oriented towards zinc with no choline being present in the active sites pocket. Other molecules are omitted for better visibility.

10. References

1. J. P. Bittner, N. Zhang, L. Huang, P. Domínguez de María, S. Jakobtorweihen and S. Kara, *Green Chem.*, 2022, **24**, 1120–1131.
2. M. J. Abraham, T. Murtola, R. Schulz, S. Páll, J. C. Smith, B. Hess and E. Lindahl, *SoftwareX*, 2015, **1**, 19–25.
3. H. Bekker, H. Berendsen, E. Dijkstra, S. Achterop, R. Vondrumen, D. Vanderspoel, A. Sijbers, H. Keegstra and M. Renardus, eds. R. A. DeGroot and J. Nadrchal, World Scientific Publishing, Singapore, 1993, pp. 252–256.
4. D. v. d. Spoel, E. Lindahl, B. Hess and t. G. d. team, GROMACS User Manual version 2019, http://www.gromacs.org).
5. J. Huang, S. Rauscher, G. Nawrocki, T. Ran, M. Feig, B. L. de Groot, H. Grubmuller and A. D. MacKerell, Jr., *Nat. Methods*, 2017, **14**, 71–73.
6. S. Jo, T. Kim, V. G. Iyer and W. Im, *J. Comput. Chem.*, 2008, **29**, 1859–1865.
7. J. Lee, X. Cheng, J. M. Swails, M. S. Yeom, P. K. Eastman, J. A. Lemkul, S. Wei, J. Buckner, J. C. Jeong, Y. Qi, S. Jo, V. S. Pande, D. A. Case, C. L. Brooks, 3rd, A. D. MacKerell, Jr., J. B. Klauda and W. Im, *J. Chem. Theory Comput.*, 2016, **12**, 405–413.
8. J. Lee, M. Hitzenberger, M. Rieger, N. R. Kern, M. Zacharias and W. Im, *J. Chem. Phys.*, 2020, **153**, 035103.
9. S. Kim, J. Lee, S. Jo, C. L. Brooks, 3rd, H. S. Lee and W. Im, *J. Comput. Chem.*, 2017, **38**, 1879–1886.
10. K. Vanommeslaeghe, E. Hatcher, C. Acharya, S. Kundu, S. Zhong, J. Shim, E. Darian, O. Guvench, P. Lopes, I. Vorobyov and A. D. Mackerell, Jr., *J. Comput. Chem.*, 2010, **31**, 671–690.
11. W. Yu, X. He, K. Vanommeslaeghe and A. D. MacKerell, Jr., *J. Comput. Chem.*, 2012, **33**, 2451–2468.
12. A. D. MacKerell, D. Bashford, M. Bellott, R. L. Dunbrack, J. D. Evanseck, M. J. Field, S. Fischer, J. Gao, H. Guo, S. Ha, D. Joseph-McCarthy, L. Kuchnir, K. Kuczera, F. T. Lau, C. Mattos, S. Michnick, T. Ngo, D. T. Nguyen, B. Prodhom, W. E. Reiher, B. Roux, M. Schlenkrich, J. C. Smith, R. Stote, J. Straub, M. Watanabe, J. Wiorkiewicz-Kuczera, D. Yin and M. Karplus, *J. Phys. Chem. B*, 1998, **102**, 3586–3616.
13. J. P. Bittner, L. Huang, N. Zhang, S. Kara and S. Jakobtorweihen, *J. Chem. Theory Comput.*, 2021, **17**, 5322–5341.
14. L. Huang, J. P. Bittner, P. Domínguez de María, S. Jakobtorweihen and S. Kara, *ChemBioChem*, 2020, **21**, 811–817.
15. L. Martínez, R. Andrade, E. G. Birgin and J. M. Martínez, *J. Comput. Chem.*, 2009, **30**, 2157–2164.

16. G. Bussi, D. Donadio and M. Parrinello, *J. Chem. Phys.*, 2007, **126**, 014101.
17. R. W. Hockney, *Methods Comput. Phys.* , 1970, **9**, 135–211.
18. H. J. C. Berendsen, J. P. M. Postma, W. F. Vangunsteren, A. Dinola and J. R. Haak, *J. Chem. Phys.*, 1984, **81**, 3684–3690.
19. M. Parrinello and A. Rahman, *J. Appl. Phys.*, 1981, **52**, 7182–7190.
20. R. Meijers, R. J. Morris, H. W. Adolph, A. Merli, V. S. Lamzin and E. S. Cedergren-Zeppezauer, *J. Biol. Chem.*, 2001, **276**, 9316–9321.
21. J. N. Dahanayake, D. N. Gautam, R. Verma and K. R. Mitchell-Koch, *Mol. Simul.*, 2016, **42**, 1001–1013.
22. A. R. Leach, *Molecular modelling: principles and applications*, Prentice Hall, 2001.
23. S. Miyamoto and P. A. Kollman, *J. Comput. Chem.*, 1992, **13**, 952–962.
24. B. Hess, H. Bekker, H. J. C. Berendsen and J. G. E. M. Fraaije, *J. Comput. Chem.*, 1997, **18**, 1463–1472.
25. W. Humphrey, A. Dalke and K. Schulten, *J. Mol. Graphics*, 1996, **14**, 33–38.
26. O. Beckstein, VMD - Visual Molecular Dynamics, http://www.ks.uiuc.edu/Research/vmd/).
27. J. P. Bittner, N. Zhang, P. Domínguez de María, I. Smirnova, S. Kara and S. Jakobtorweihen, *J. Phys. Chem. B*, 2025, **129**, 1197–1213.
28. Y. Sugita, A. Kitao and Y. Okamoto, *J. Chem. Phys.*, 2000, **113**, 6042–6051.
29. J. Kastner and W. Thiel, *J. Chem. Phys.*, 2005, **123**, 144104.
30. J. Kastner and W. Thiel, *J. Chem. Phys.*, 2006, **124**, 234106.